

## *d*-Band Quantum Well States

D.-A. Luh,<sup>1,2</sup> J.J. Paggel,<sup>3</sup> T. Miller,<sup>1,2</sup> and T.-C. Chiang<sup>1,2</sup>

<sup>1</sup>*Department of Physics, University of Illinois, 1110 West Green Street, Urbana, Illinois 61801-3080*

<sup>2</sup>*Frederick Seitz Materials Research Laboratory, University of Illinois, 104 South Goodwin Avenue, Urbana, Illinois 61801-2902*

<sup>3</sup>*Freie Universität Berlin, Institut für Experimentalphysik, 14195 Berlin, Germany*

(Received 14 December 1999)

Observations of *d*-band quantum well states are made for atomically uniform Ag films on Fe(100) using angle-resolved photoemission. For increasing film thicknesses, quantum well peaks within the small *4d* bandwidth multiply rapidly and merge into a bulklike spectrum at  $\sim 25$  monolayers. An analysis of the peak positions yields a highly accurate bulk band structure of Ag. A very narrow *d*-band peak width (13 meV) is observed at the band top.

PACS numbers: 73.20.Dx, 73.61.At, 79.60.Dp

The possibility of *d* electrons in a film forming quantum well states is an interesting issue both conceptually and experimentally. While there are numerous reports of angle-resolved photoemission studies of quantum well states derived from the nearly free electron like *sp* electrons [1,2], there have been no comparably detailed studies involving the *d* electrons. The *d* electrons have a more compact wave function near the atomic core, experience a larger correlation effect, and have much smaller energy dispersions and group velocities. Strong Coster-Kronig-Auger decay causes the *d*-state lifetime to be generally short, and the mean free path, being the product of the group velocity and the lifetime, is also short. As a result, the *d* wave functions are much more localized, and quantum well effects should diminish when the film thickness becomes larger than the mean free path. From the experimental point of view, *d*-band quantum well states are hard to observe for yet another reason. Many (typically five) *d* bands coexist in a small bandwidth, within which each band gives rise to  $\sim N$  quantum well states, where  $N$  is the number of atomic layers in the film. Taking Ag as an example, the *4d* shell is almost like a shallow core level. The bandwidth is just under 4 eV, within which there would be  $\sim 100$  quantum well states for a 20-monolayer (ML) film. Most of these would be significantly lifetime broadened and, therefore, unlikely to be resolved. Yet *d*-band quantum well states can be extremely important for magnetic coupling effects in transition metal film structures, which are finding useful applications in areas of magnetic recording and “spintronics” (electronics based on the spin rather than the charge of carriers) [2–8]. This Letter presents a study of the basic properties of *d*-band quantum well states that should serve as a baseline for future technological development based on quantum coherence and interference of *d* wave functions. Our analysis also yields a highly accurate bulk band structure of Ag covering a wide energy range as well as useful information about the lifetime broadening.

In order to resolve the many possible *d* states in a film, it is important to eliminate extrinsic peak broadening. The most common problem is film roughness. In our work, we

employ atomically uniform films of Ag grown on a Fe(100) whisker [1]. Photoemission from these “perfect” films shows discrete layer-by-layer quantum well peak evolution, and the absence of atomic layer fluctuation is key to the success of our study. The photoemission measurements were carried out at the Synchrotron Radiation Center in Stoughton, Wisconsin, which is managed by the University of Wisconsin-Madison as a national user facility. An undulator-based plane-grating monochromator and a 4-m normal-incidence monochromator provided the photon beam. Normal-emission spectra for photon energies in the range of 12–80 eV were collected using a hemispherical analyzer. Because of large variations in peak cross section, this wide energy range allowed a better determination of closely spaced peak positions (see below). A liquid nitrogen cryostat kept the sample at 110 K during the measurements.

Figure 1 shows some sample data taken with photon energies of 35 and 60 eV for various film thicknesses as indicated. A number of well separated, periodic peaks are

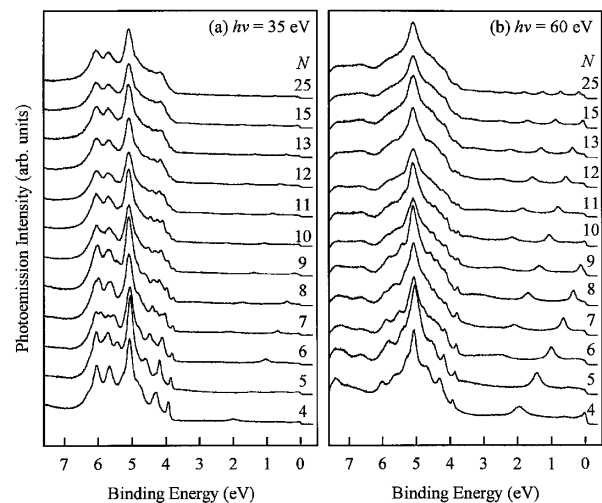


FIG. 1. Normal emission spectra taken with (a)  $h\nu = 35$  eV and (b)  $h\nu = 60$  eV. The layer thicknesses  $N$  in terms of monolayers are indicated.

seen within the binding energy range of 0–3 eV, which are quantum well states derived from the nearly free electron like  $sp$  band [1]. These peaks are easily seen for  $h\nu = 60$  eV and are much weaker for  $h\nu = 35$  eV due to lower cross sections. The peak positions are independent of photon energy, and the energy shift of each peak caused by a thickness increment of 1 ML is fairly large due to a large  $sp$ -band group velocity. All of the spectra shown in Fig. 1 correspond to atomically uniform films. At noninteger coverages, the spectrum would show two sets of peaks corresponding to neighboring integer thicknesses.

The  $d$ -band region begins at  $\sim 4$  eV binding energy, and there are numerous quantum well peaks in Fig. 1. These data as well as data taken with other photon energies and other thicknesses yield the following observations: (i) The number of peaks in the  $d$ -band region,  $\sim 5N$ , increases rapidly as a function of thickness, and eventually the peaks can no longer be resolved. Even at a film thickness of just 4 ML, up to  $\sim 20$  peaks are expected. (ii) While the energy position of each peak is independent of the photon energy, the cross section can vary significantly. Some weaker peaks that are not apparent in the data shown in Fig. 1 can be brought out by using different photon energies, thus allowing a better compilation of peak positions. (iii) The peaks near the top of the  $d$ -band manifold are much sharper than the rest. The leading peaks remain well resolved for most of the thickness range studied. (iv) At film thicknesses larger than  $\sim 25$  ML, the large number of peaks (over 100) merges into a bulklike spectrum.

The quantum well peak positions, wherever resolvable, are deduced from a fit to the spectra using Voigt line shapes. The Gaussian width is the instrumental resolution deduced from a fit to the Fermi edge line shape, and the Lorentzian width is taken to be a fitting parameter. The resulting compilation of peak positions allows us to refine the band structure, which is known only approximately from various calculations and experiments based on bulk samples. The basis of this analysis [9–11] is the Bohr-Sommerfeld quantization rule, also known as the phase accumulation rule:

$$2kNt + \Phi = 2n\pi, \quad (1)$$

where  $k$  is the wave vector of the quantum well state,  $t$  is the monolayer thickness,  $\Phi$  is the total boundary phase shift, and  $n$  is a quantum number. The binding energy  $E$  of each quantum well peak is directly measured, but Eq. (1) in itself is insufficient to give  $k$ , because  $\Phi$  is unknown. At least another thickness  $N'$  is required. For example, if state  $n'$  for thickness  $N'$  is at the same binding energy, then  $k$  and  $\Phi$  are the same, and the quantization condition for this state,

$$2kN't + \Phi = 2n'\pi, \quad (2)$$

can be combined with Eq. (1) for a simultaneous solution of  $k$  and  $\Phi$  at  $E$ .

Instead of a point-by-point analysis, we employ a least-squares fitting procedure to account for all measured peak

positions obtained at many different film thicknesses. A parametrized band structure  $k(E)$  based on the combined interpolation scheme of Smith and Mattheiss [12] is used. The phase shift function  $\Phi(E)$  is taken to be a third order polynomial with its coefficients as fitting parameters. Using these fitting functions, quantum well peak positions are calculated numerically as solutions of Eq. (1) for different values of  $n$  and compared with the positions of resolved peaks in the data. The fitting parameters in the functions  $k(E)$  and  $\Phi(E)$  are then varied for a best fit. Excluded from this fit are data for  $N = 1, 2$ , and 3 because Eq. (1) is not expected to work well at such small thicknesses, where the potential steps at the two boundaries of the film overlap and the phase shift becomes dependent on the film thickness [1].

Figure 2(a) shows an amplified portion of the 35-eV data set together with the predicted peak positions based on the best fit, using various symbols. The different colors denote quantum well peaks derived from the correspondingly color-coded bands shown in Fig. 2(b). Each colored curve marked  $n$  in Fig. 2(a) corresponds to a fixed quantum

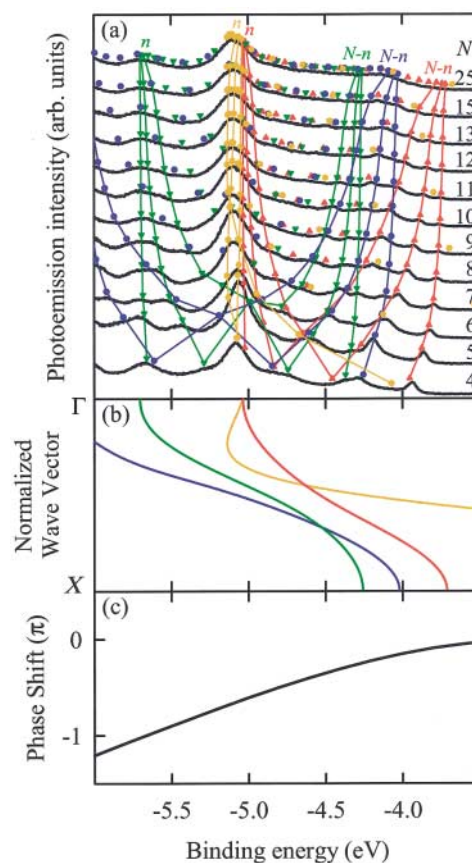


FIG. 2 (color). (a) Normal emission spectra taken with  $h\nu = 35$  eV for various film thicknesses  $N$ . Quantum well peak positions based on our model fit are shown using symbols with different colors. Each colored curve connects quantum well peaks of the same (reduced) quantum number for different thicknesses, and only small (reduced) quantum numbers are included. (b) Band dispersions from the best fit. The colors correspond to the symbols in (a). (c) The phase shift function from the best fit.

number  $n$  (1, 2, or 3) in Eq. (1). For quantum well peaks with  $k$  near the zone boundary, it is more convenient to use a reduced quantum number  $N - n$  (corresponding to using a reduced wave vector measured from the zone boundary). Each colored curve in Fig. 2(a) marked by  $N - n$  corresponds to quantum well states with a fixed reduced quantum number (0, 1, or 2). Clearly, there are many more peaks at higher thicknesses as the allowed quantum numbers increase, and gradually the peaks become unresolvable. By  $N = 25$ , the peaks, lifetime broadened, merge to form essentially a continuum. The spectrum becomes bulklike and changes little at higher thicknesses. Thus, quantum well effects are important only up to about 25 ML. Figure 2(c) shows the phase shift from the fit.

Figure 3 shows in detail the resulting band structure from our analysis (solid curves). The three shaded regions indicate where data are available. The bottom shaded region covers the  $d$  manifold and corresponds to the analysis discussed above. Also included in our fit of the band structure is the  $sp$  quantum well data previously analyzed [1]; the range of this data set covers 0–2 eV below the Fermi level and is indicated by the middle shaded region. There are no data points between 2 and  $\sim 4$  eV below the Fermi level, because the  $sp$  band is not confined resulting in no quantum well peaks. A portion of the unoccupied

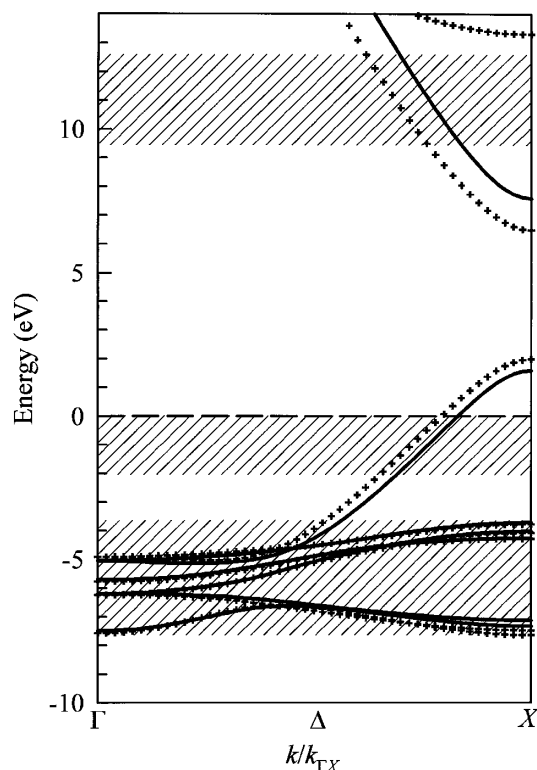


FIG. 3. The band structure of Ag along [100] based on a best fit to our experimental results (solid curves). The shaded regions indicate energy ranges where data are available. The crosses are taken from the work of Smith [13] based on a fit to old photoemission and optical data using a combined interpolation scheme. The Fermi level is indicated by a horizontal dashed line.

$sp$  band, deduced from direct-transition data taken from a bulk single crystal Ag(100) [1], was also included in the fit as indicated by the top shaded region. For comparison, the band structure proposed by Smith [13] based on an analysis of old photoemission and optical data is included in Fig. 3 as crosses. Accurate band mapping is a well-known challenge for conventional photoemission studies using bulk samples due to a poor  $k$  resolution caused by a very large final state lifetime broadening. This problem does not exist for the present study because  $k$  is defined by the quantum well geometry.

An inspection of the spectra in Figs. 1 and 2 reveals that the widths of the  $d$ -band quantum well peaks increase significantly from the top to the bottom of the  $d$ -band manifold. This trend is further illustrated by the spectra shown in Fig. 4(a), taken with a photon energy of 12 eV. As expected, the lifetime broadening increases towards higher binding energies, because there is more phase space for a  $d$  hole to decay via  $d$ - $d$ - $sp$  Coster-Kronig-Auger transitions. This decay channel is, however, inoperative for the leading peak near the top of the  $d$  manifold, and therefore this peak remains very sharp for most of the thickness range studied before it weakens and merges with other peaks. The circles in Fig. 4(b) represent the Lorentzian width of the leading peak plotted as a function of film thickness for various photon energies. The width is seen to decrease steadily for increasing film thickness, reaching a minimum value of  $\sim 20$  meV around 15 ML, beyond which the peak becomes too weak for a reliable analysis.

The reason for this thickness dependence is as follows. The lack of a true gap in the Fe substrate leads to a boundary reflectivity  $R < 1$ , and the quantum well states in the Ag film are not fully confined. Partial reflection at the boundary results in decay of the wave function and, hence, in a broadening beyond the lifetime contribution  $\Gamma$ . This effect is particularly important at small thicknesses because there will be more reflections of the electrons at the boundaries. A straightforward analysis [1] shows that the peak width is given by

$$\delta E = \Gamma \frac{\lambda}{Nt} \frac{1 - R \exp(-Nt/\lambda)}{\sqrt{R} \exp(-Nt/2\lambda)}, \quad (3)$$

where  $\lambda$ , the mean free path, is related to  $\Gamma$  and the group velocity  $v$  by  $\lambda = \hbar v/\Gamma$ . The solid curve in Fig. 4(b) is a fit with  $\Gamma = 13$  meV and  $R = 0.68$  as the only fitting parameters. This  $\Gamma$  represents by far the narrowest lifetime width ever reported for a bulk state at such a large binding energy (4 eV). For comparison, the narrowest *surface* state ever reported was the  $\bar{M}$  state on Cu(100) with a width of 7 meV at a binding energy of 1.8 eV [14]. Such surface states tend to be narrow because the wave functions are spatially decoupled from the bulk resulting in a suppressed Auger decay rate. The narrowest bulk  $d$  state ever reported previously was from the top of the  $d$  band of Cu(100) with a width of about 25 meV at a binding energy of 2 eV [15].

Contributions to this  $\Gamma$  include phonon scattering and  $d$ - $sp$ - $sp$  Auger decay (which is much weaker than the

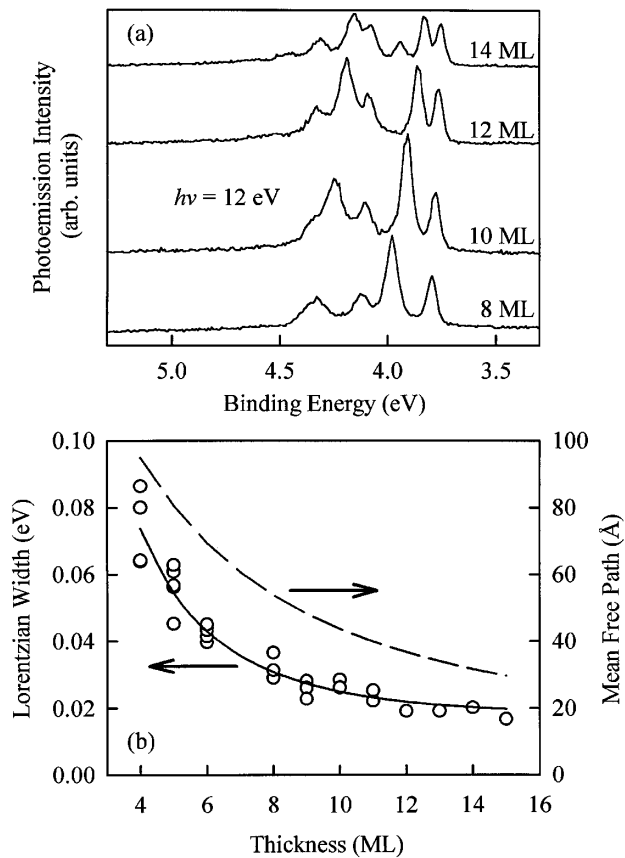


FIG. 4. (a) Normal emission spectra taken with  $h\nu = 12$  eV for various layer thicknesses as indicated. (b) The circles are Lorentzian linewidths of the leading  $d$  quantum well peak as a function of film thickness. Several data points may be present at the same thickness, and these are results from different photon energies. The solid curve is a fit. The dashed curve shows the corresponding mean free path.

$d$ - $d$ - $sp$  channel). Note that as the film thickness increases, the leading  $d$  quantum well peak moves ever closer to the band edge. As the group velocity decreases, so does the mean free path  $\lambda = \hbar v / \Gamma$  for a constant lifetime width  $\Gamma = 13$  meV. The mean free path calculated using the best-fit band structure is shown as a dashed curve in Fig. 4(b). At a film thickness of 15 ML,  $\lambda = 30$  Å is just about the same as the film thickness. Beyond this point, quantum well effects should diminish rapidly because of the loss of phase coherence. This partly explains the very much reduced quantum well peak intensity beyond this thickness. Defect scattering is negligible in this case, because the mean free path caused by defect scattering alone, about 1000 Å [1], is much larger than  $\lambda$ .

From this study, we can conclude that  $d$ -band quantum well states do exist despite the relatively localized nature of the  $d$  states. However, the thickness range in which quantum well effects are significant is limited to  $\sim 25$  ML, much smaller than that for the  $sp$  states (well over 100 ML) [1]. Within the  $d$  manifold, lifetime broadening becomes larger towards higher binding energies, fur-

ther limiting the range of quantum well effects. Despite the large number of peaks crowding the  $d$  manifold, it is possible to perform a detailed analysis of the peak positions by taking measurements over a wide range of photon energy. Such an analysis yields a very accurate band structure as well as valuable information about the lifetime, which is difficult to obtain using traditional photoemission measurements of bulk crystals.

This material is based upon work supported by the U.S. National Science Foundation, under Grants No. DMR-99-75470 and No. DMR-99-75182. An acknowledgment is made to the Donors of the Petroleum Research Fund, administered by the American Chemical Society and to the U.S. Department of Energy, Division of Materials Sciences (Grant No. DEFG02-91ER45439) for partial support of the synchrotron beam line operation and for support of the central facilities of the Materials Research Laboratory. The Synchrotron Radiation Center of the University of Wisconsin is supported by the National Science Foundation under Grant No. DMR-95-31009.

- [1] J.J. Paggel, T. Miller, and T.-C. Chiang, Phys. Rev. Lett. **81**, 5632 (1998); Science **283**, 1709 (1999); Phys. Rev. B (to be published).
- [2] R. K. Kawakami, E. Rotenberg, H. J. Choi, E. J. Escorcia-Aparicio, M. O. Bowen, J. H. Wolfe, E. Arenholz, Z. D. Zhang, N. V. Smith, and Z. Q. Qiu, Nature (London) **398**, 132 (1999).
- [3] P. Grunberg, R. Schreiber, Y. Pang, M. B. Brodsky, and H. Sowers, Phys. Rev. Lett. **57**, 2442 (1986).
- [4] S. S. P. Parkin, N. More, and K. P. Roche, Phys. Rev. Lett. **64**, 2304 (1990).
- [5] J. E. Ortega and F. J. Himpsel, Phys. Rev. Lett. **69**, 844 (1992).
- [6] D. Hartmann, W. Weber, A. Rampe, S. Popovic, and G. Güntherodt, Phys. Rev. B **48**, 16 837 (1993).
- [7] D. Li, J. Pearson, S. D. Bader, E. Vescovo, D.-J. Huang, P. D. Johnson, and B. Heinrich, Phys. Rev. Lett. **78**, 1154 (1997).
- [8] P. D. Johnson, Rep. Prog. Phys. **60**, 1217 (1997).
- [9] S. Å. Lindgren and L. Walldén, J. Phys. Condens. Matter **1**, 2151 (1989).
- [10] M. A. Mueller, T. Miller, and T.-C. Chiang, Phys. Rev. B **41**, 5214 (1990).
- [11] N. V. Smith, N. B. Brookes, Y. Chang, and P. D. Johnson, Phys. Rev. B **49**, 332 (1994).
- [12] N. V. Smith and L. F. Mattheiss, Phys. Rev. B **9**, 1341 (1974).
- [13] N. V. Smith, Phys. Rev. B **9**, 1365 (1974); **9**, 5019 (1974); R. L. Benbow and N. V. Smith, Phys. Rev. B **27**, 3144 (1983).
- [14] D. Purdie, M. Hengsberger, M. Garnier, and Y. Baer, Surf. Sci. **407**, L671 (1998).
- [15] R. Matzdorf, A. Gerlach, F. Theilmann, G. Meister, and A. Goldmann, Appl. Phys. B **68**, 393 (1999).